Chaotic synchronizations of spatially extended systems as nonequilibrium phase transitions

M. Cencini,[1] C. J. Tessone,[2] and A. Torcini[3]
[1]*INFM-CNR, SMC Dipartimento di Fisica, Università Roma 1, P.zzle A. Moro 2, 00185 Roma, Italy and Istituto dei Sistemi Complessi-CNR, via dei Taurini 19, 00185 Roma, Italy*
[2]*Chair of Systems Design, ETH Zürich, Kreuzplatz 5, 8037 Zürich, Switzerland*
[3]*INFN-Sezione di Firenze and CSDC, via Sansone 1, 50019 Sesto Fiorentino, Italy, Centre de Physique Théorique, Campus de Luminy, 13288 Marseille, France, and Istituto dei Sistemi Complessi-CNR, via Madonna del Piano 10, 50019 Sestio Fiorentino, Italy*

(Received 21 February 2008; accepted 28 May 2008; published online 22 September 2008)

Two replicas of spatially extended chaotic systems synchronize to a common spatio-temporal chaotic state when coupled above a critical strength. As a prototype of each single spatio-temporal chaotic system a lattice of maps interacting via power-law coupling is considered. Furthermore, each unit in the one-dimensional chain is linked to the corresponding one in the replica via a local coupling. The synchronization transition is studied as a nonequilibrium phase transition, and its critical properties are analyzed at varying the spatial interaction range as well as the nonlinearity of the dynamical units composing each system. In particular, continuous and discontinuous local maps are considered. In both cases the transitions are of the second order with critical indices varying with the exponent characterizing the interaction range. For discontinuous maps it is numerically shown that the transition belongs to the anomalous directed percolation (ADP) family of universality classes, previously identified for Lévy-flight spreading of epidemic processes. For continuous maps, the critical exponents are different from those characterizing ADP, but apart from the nearest-neighbor case, the identification of the corresponding universality classes remains an open problem. Finally, to test the influence of deterministic correlations for the studied synchronization transitions, the chaotic dynamical evolutions are substituted by suitable stochastic models. In this framework and for the discontinuous case, it is possible to derive an effective Langevin description that corresponds to that proposed for ADP. © *2008 American Institute of Physics*.
[DOI: 10.1063/1.2945903]

Synchronization is ubiquitous in nature; neuronal populations, cardiac pacemakers, Josephson circuits, and even coupled chaotic systems can synchronize during their activity. Remarkably, all these different phenomena can be described within a common framework represented by nonlinear dynamics.[1] Synchronization of spatially extended chaotic systems is particularly interesting as it allows for transferring concepts and methods borrowed from statistical mechanics to nonlinear dynamics. Indeed, a direct connection between the critical properties of nonequilibrium phase transitions and synchronization processes has been established.[2,3] Noticeably, for diffusively coupled chaotic systems only two universality classes, Directed Percolation and Multiplicative Noise, encompass all the synchronization transitions. Originally these classes have been identified in completely different contexts such as epidemics spreading and pinning/depinning of interfaces to/from a substrate.[4,5] The parallel between nonequilibrium critical phenomena and synchronization processes is possible only thanks to the erratic nature of the synchronized state, where chaos somehow mimics the presence of thermal noise in real systems. In this paper we propose an extension of such an analogy to synchronization transitions of long-range coupled systems. Long-range interactions naturally appears in many circumstances ranging from neuronal networks to solid state physics. Therefore, a characterization of these transitions is definitely worthy and of interest for a wide scientific community.

I. INTRODUCTION

Since its discovery,[6] chaotic synchronization is a very active and important field of research,[1] with applications in such diverse fields as secure communications,[7,8] semiconductor lasers,[9] chemical reactions,[10] living systems,[11] and electrically coupled neurons *in vitro*.[12]

The phenomenology of the synchronization transition (ST) is particularly rich for spatially extended chaotic systems, where a parallel with critical phenomena can be drawn.[13] In the last decade, an ongoing research activity has been devoted to relate chaotic STs to nonequilibrium phase transitions.[2,3,14–24] Nowadays, it is well established that the synchronization of two replicas of a chaotic system coupled via the same realization of spatio-temporal noise,[2] or by coupling corresponding elements of the replicas via a local interaction,[3] can be characterized as a continuous nonequilibrium transition from an active to an absorbing phase. In systems with nearest-neighbor (NN) couplings, it has been found that the STs belong to two universality classes, depending on the local dynamical features, namely, directed

percolation (DP) (Refs. 4 and 25) or multiplicative noise (MN).[5] These studies have been mainly performed for coupled map lattices (CML), which are prototype models for systems exhibiting spatio-temporal chaos.[26] A dynamical order parameter able to locate the synchronization transitions (ST) is represented by the propagation velocity of information V_I, Refs. 28 and 29; in the synchronized (resp. desynchronized) state this quantity is zero (resp. finite). Moreover, for continuous maps, where the dynamics is dominated by linear effects, V_I vanishes together with the transverse Lyapunov exponent. Therefore, a characterization of the synchronization phenomenon in terms of linearized equations (corresponding to a Lyapunov analysis) is sufficient to properly locate the STs. In this case the critical indexes associated to the ST are of the MN kind.[3] On the other hand, for discontinuous (or quasi-discontinuous[27]) maps, due to the predominance of nonlinear effects, the replicas synchronize for definitely negative transverse Lyapunov exponents.[2,29] For these maps the ST cannot be anymore described within a linear framework and the transition is now characterized by critical properties typical of DP, analogously to what happens for cellular automata.[22,30] These findings have been also confirmed by the analysis of stochastic models mimicking the synchronization of continuous/discontinuous maps.[17]

Recently, synchronization has also been studied for chaotic systems presenting long-range interactions, which are relevant to many real contexts, such as disease spread via aviation traffic,[31] neuron populations,[32] Josephson junctions,[33] and cardiac pacemaker cells.[34]

Typically, long-range interactions are introduced by considering CMLs with coupling decaying as a power law.[21,35–37] In such a model, when the local dynamics is dominated by nonlinear mechanisms, the STs have been shown to belong to a family of universality classes known as anomalous directed percolation (ADP).[24,38] ADP has been previously identified for epidemic spreading whenever the infective agent can perform unrestricted Lévy flights.[39,40] Such processes, originally introduced in Ref. 41, can be modeled by assuming, e.g., in $d=1$, that the disease propagates from an infected site to any other with a probability $P(r)\sim r^{-(1+\sigma)}$ algebraically decaying with the spatial distance r, where σ controls the interaction range. Hinrichsen and Howard have numerically shown for a stochastic lattice model (generalizing directed bond percolation) that the critical exponents vary continuously with σ.[40] These findings confirm previous theoretical results[39] indicating that usual DP should be recovered for sufficiently short-ranged coupling [namely, $\sigma>\sigma_c\equiv 2.0677(2)$] and that a mean-field description should become exact for $\sigma<\sigma_m\equiv 0.5$ (for a recent and exhaustive review, see Ref. 38).

In this paper, we first reconsider, by performing more accurate estimations of the critical exponents, the results obtained for NN interactions both for deterministic as well as for stochastic local dynamics.[16,17] Then we focus on the synchronization transition in systems with power-law coupling. In this context we extend previous analysis for discontinuous deterministic maps[24] to a stochastic version of the model, and we confirm that whenever the STs are driven by nonlinear effects the associated critical properties belong to the anomalous directed percolation universality classes. Finally, we present a first evaluation of the critical properties of the synchronization transitions for continuous chaotic maps with power-law interactions.

The paper is organized as follows: The employed deterministic and stochastic models are introduced in the next section, while Sec. III is devoted to the methods used to study their critical properties. In Sec. IV, STs are reexamined for nearest-neighbor interacting systems; while Sec. V is focused on power-law coupled systems. Conclusions and perspectives are discussed in Sec. VI. The Appendix presents a derivation of the field equation, known to reproduce ADP critical phenomena, for the stochastic model with power-law interactions.

II. MODELS

In this paper we investigate the synchronization between two replicas of CMLs transversally coupled according to the following scheme:

$$\begin{aligned} x_i(t+1) &= (1-\gamma)F[\tilde{x}_i(t)] + \gamma F[\tilde{y}_i(t)], \\ y_i(t+1) &= (1-\gamma)F[\tilde{y}_i(t)] + \gamma F[\tilde{x}_i(t)], \end{aligned} \tag{1}$$

where $i=1,\ldots,L$ is the discrete spatial index with L denoting the system size; $x_i(t), y_i(t)\in[0:1]$ are the state variables, and periodic boundary conditions are used ($x_{L+1}=x_1$); $F(x)$ determines the local dynamics on each site of the lattice (see below for its specification). The parameter γ sets the strength of the site-by-site coupling between the two replicas.

The variables $\tilde{z}_i\in\{\tilde{x}_i,\tilde{y}_i\}$ indicate spatially averaged quantities. In particular, two different kind of spatial averages are introduced to reproduce short– and long-ranged interactions. The former represents a discretized version of spatial diffusion among nearest neighbor sites and reads

$$\tilde{z}_i = (1-\epsilon)z_i + \frac{\epsilon}{2}(z_{i-1}+z_{i+1}), \tag{2}$$

where ϵ measures the intensity of the diffusive interaction within each replica. The latter is obtained by considering a coupling decaying as a power law,[21,35,37] i.e.,

$$\tilde{z}_i = (1-\epsilon)z_i + \frac{\epsilon}{\eta(\sigma)}\sum_{k=1}^{L'}\frac{z_{i-k}+z_{i+k}}{k^{1+\sigma}}, \tag{3}$$

where σ tunes the interaction range (the rationale for defining the exponent as $1+\sigma$ will become clear in Sec. V). For $\sigma\to\infty$, Eq. (3) reduces to the diffusive case Eq. (2), while for $\sigma=-1$ it corresponds to the mean-field coupling, usually employed in the study of globally coupled maps.[42] Actually, as discussed in Ref. 21, the large scale properties of the system should coincide with those at $\sigma=0$ for any $\sigma\in[-1:0]$. Since the sum extends up to $L'=(L-1)/2$ the model is well defined only for odd L-values, and $\eta(\sigma)=2\sum_{k=1}^{L'}k^{-(1+\sigma)}$ is a normalization factor to ensure that $\tilde{z}\in[0:1]$. For both kinds of coupling Eqs. (2) and (3), periodic boundary conditions are assumed and the diffusive coupling ϵ is set to $2/3$. Notice that the results do not seem to depend on the chosen value of ϵ.

Several studies[2,3,17,21,28] have shown that the system dynamics is strongly influenced by the continuity properties of the local map $F(x)$.[29] In particular, the spatio-temporal propagation of disturbances[28] and the properties of synchronization[3] are noticeably different if the map is continuous or (quasi) discontinuous. For this reason, throughout this work, we consider two different deterministic maps: The Bernoulli map $F(x)=2x(\mathrm{mod}\ 1)$, which is characterized by a discontinuity making dominant the nonlinear effects, and the tent map $F(x)=1-2|x-1/2|$, whose dynamical properties are well captured by linear analysis.

The synchronization transition is observed while increasing the coupling γ: Above a critical value γ_c the two replicas synchronize onto the same chaotic trajectory. In other words, for $\gamma \gtrsim \gamma_c$ the synchronization error $w_i(t)=|x_i(t)-y_i(t)|$ vanishes for sufficiently long times.

Parallel to Eq. (1), we also consider a stochastic model which mimics the evolution of the synchronization error (difference field) $w_i(t)$ in proximity of the ST. Stochastic dynamics is expected to deplete the role played by spatio-temporal correlations, unavoidable in deterministic systems, and thus should allow more accurate estimations of the critical exponents.

In particular, we consider a stochastic model able to reproduce the main features of ST both for continuous and discontinuous maps. We consider the so-called random multiplier model, originally proposed in Refs. 16 and 17. The quantity $w_i(t)$ defined in each site of the chain evolves according to the following stochastic dynamics:

$$w_i(t+1)=\begin{cases}1, & \text{w.p. } p=a\tilde{w}_i(t)\\ a\tilde{w}_i(t), & \text{w.p. } 1-p\end{cases} \quad \text{if } \tilde{w}_i(t)>\Delta, \tag{4}$$

$$w_i(t+1)=\begin{cases}\tilde{w}_i(t)/\Delta, & \text{w.p. } p=a\Delta\\ a\tilde{w}_i(t), & \text{w.p. } 1-p\end{cases} \quad \text{if } \tilde{w}_i(t)\le\Delta, \tag{5}$$

where $w_i(t)\in[0:1]$ and $\tilde{w}_i$ indicates the spatial averages that depending on the nature of the coupling, NN or long-range, is given by Eq. (2) or (3). The parameter Δ controls the nonlinear effects, while a the linear ones. For the local maps considered in this article a can be identified with $2(1-2\gamma)$.[17] Therefore, to vary the coupling γ in the deterministic model amounts to modify a in the stochastic one. Notice that, due to the relationship between the parameters γ and a, in the random multiplier model to achieve synchronization a should be reduced. For sufficiently small (resp. large) Δ the models (4) and (5) mimic the dynamics of (quasi)-discontinuous (resp. continuous) maps, where nonlinear (resp. linear) effects are predominant. Following Ref. 17, in order to reproduce the behaviors of the Bernoulli or of continuouslike maps we fixed $\Delta=0$ or $\Delta=0.2$, respectively.

III. CHARACTERIZATION OF THE SYNCHRONIZATION TRANSITIONS

The phenomenology of the synchronization transitions at varying the coupling range and the type of local dynamics can be visualized by looking at Fig. 1. The figure displays the difference field $w_i(t)$ for various values of σ with transversal coupling just above the synchronization transition ($\gamma \gtrsim \gamma_c$) for Bernoulli as well as for tent maps. The spatio-temporal evolution of $w_i(t)$ is strongly dependent not only on the continuous/discontinuous nature of the local dynamics, but also on the interactions range within each replica. For the discontinuous maps [Figs. 1(a)–1(d)], percolating structures are clearly visible in the short-range limit (i.e., large σ). However, as the range of the interaction increases (i.e., σ decreases) these spatial structures tend to be smoothed out and, finally, for $\sigma \lesssim 0.5$, they are no more detectable. When the local dynamics is governed by a continuous map, the qualitative results change completely [Figs. 1(e)–1(h)]. In this case, desynchronization (resurgence) phenomena are possible within the already synchronized areas and this leads to a less defined distinction between synchronized and desynchronized regions. However, a disappearance of the spatial structures is once more observable by increasing the interaction range.

The patterns observed in Fig. 1 suggest a link between synchronization transitions and nonequilibrium phase transitions from an active to an absorbing (quasi-absorbing) phase.[4,5] In particular, Fig. 1 recalls the patterns observed for directed percolation (DP),[4,25] a contact process usually employed in the description of epidemics spreading. DP has been the subject of active research in the last 20 years and, notwithstanding exact analytical results are still lacking, detailed numerical studies have been able to determine its critical properties up to a noticeable accuracy.[43] Quite recently, also experimental measurements of the critical DP indices have been reported for a transition to spatio-temporal intermittency in a quasi-one-dimensional system consisting of a ring of ferrofluidic spikes,[44] and for a transition between two topologically different turbulent states in a quasi-two-dimensional layer of nematic liquid crystals.[45] Figure 1(e) resembles instead surface roughening. Indeed, Kurths and Pikovsky[46] have proven that within a linear framework the evolution of the difference field of coupled CMLs is described by a Kardar–Parisi–Zhang equation[47] in the presence of a hard wall. This latter equation can be put in a direct relationship with the multiplicative noise (MN) Langevin equation,[5] which reproduce critical properties of nonequilibrium pinning-depinning as well as wetting-dewetting transitions.[19,48]

As mentioned in the Introduction, the above analogies are not merely qualitative, indeed several studies[2,3,17,18] have quantitatively shown that, depending on the prevalence of linear (resp. nonlinear) effects in the local dynamics, ST in diffusively coupled systems belongs to the MN (resp. DP) universality class. In particular, by changing the value of the local multiplier (a control parameter), one can pass continuously from one class to the other,[17] thus suggesting that both these nonequilibrium transitions can be described within a single field-theoretic framework. This is confirmed by further results reported in Ref. 19 for a microscopic model of wetting transitions and in Ref. 18 for the Kardar–Parisi–Zhang equation with an attractive wall. Indeed, for such processes the time evolution of the local density of active sites $n(x,t)$ admits a formally quite similar Langevin description,

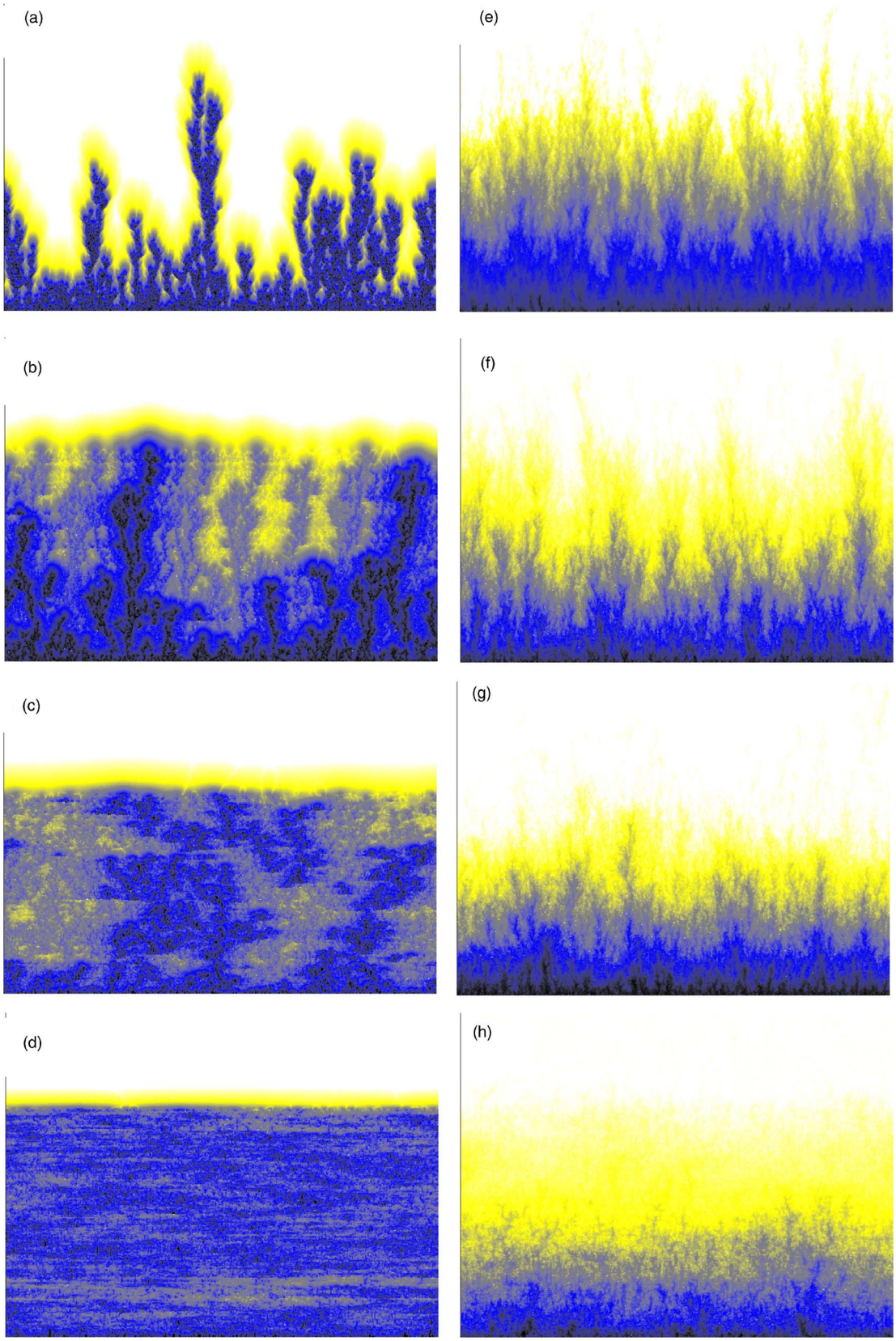

FIG. 1. (Color online) The spatio-temporal evolution of the synchronization error for power-law coupled maps is depicted for local dynamics given by the Bernoulli map [panels (a)–(d)] and the tent map [panels (e)–(f)]. Each row corresponds to different values of the exponent σ, namely, $\sigma=5$ [panels (a) and (e)]; $\sigma=2$ [panels (b) and (f)]; $\sigma=1.2$ [panels (c) and (g)] and $\sigma=0.5$ [panels (d) and (h)]. The horizontal axis represents space, while the vertical one represents time. Note that the patterns observed for NN interaction closely resembles those reported in (a) and (e) for discontinuous and continuous maps, respectively. The color code represents the synchronization error (in logarithmic scale), ranging from white $[w_i(t)\to 0]$ to black $[w_i(t)=1]$; larger values correspond to darker tones. The results reported in the panels have been obtained by employing the modified model (14) for $q=4$ and $M=5$.

$$\partial_t n = D_N \nabla^2 n + \tau n - \Gamma n^p + g(n)\xi. \tag{6}$$

Such equation recovers the Reggeon–field theory describing DP for $p=2$ and $g(n) \propto \sqrt{n}$, while the minimal model for MN can be obtained from Eq. (6) whenever $g(n) \propto n$. In the synchronization context, n represents the coarse grained synchronization error obtained by averaging $w_i(t)=|x_i(t)-y_i(t)|$ over a suitable space-time cell. The parameters entering Eq. (6) are the diffusion coefficient D_N (corresponding to ϵ); τ that measures the distance from the critical point (i.e., from the synchronization threshold γ_c) and the amplitude of the nonlinear term Γ. Finally, ξ is a zero-average δ-correlated (in space and time) Gaussian noise field with unit variance.

In Refs. 39 and 40 the field description has been extended to include long-range interactions, leading to the following stochastic equation:

$$\partial_t n = D\nabla^2 n + D_A \nabla^\sigma n + \tau n - \Gamma n^2 + g(n)\xi, \tag{7}$$

which generalizes Eq. (6) through the addition of an anomalous diffusion term with coefficient D_A and range of interaction parametrized by σ. For $g(n) \propto \sqrt{n}$, Eq. (7) describes the ADP universality class while, to the best of our knowledge, such an equation has never been studied in the context of anomalous MN, i.e., for $g(n) \propto n$.

Recently in Ref. 24 we have numerically shown that STs observed for model (1) with power law coupling Eq. (3) and equipped with discontinuous maps (namely, Bernoulli maps) belong to the ADP universality class. In this context the extension of the analysis to the stochastic models (4) and (5) would be particularly interesting, for two reasons. First, the models (4) and (5) are known to reproduce quite well the phenomenology of synchronization for systems like Eq. (1) with short-range coupling.[17] Second, after a suitable coarse-graining, such models for $\Delta=0$ are effectively described by the Langevin equation derived for Reggeon field theory, providing further support to the connection with DP.[17] Here, in the Appendix, we show that this kind of mapping can be extended also to the power-law interacting model and, in this case, Eq. (7) is recovered. Furthermore, the aim of the present work is to extend the studies reported in Ref. 24 also to continuous maps.

Before reporting a detailed analysis of the synchronization transition for the above defined models, let us introduce the exponents employed to characterize STs as nonequilibrium transitions. These are defined through the spatially averaged synchronization error $\rho_\gamma(t)=\Sigma_i w_i(t)/L$ which, at sufficiently long times, vanishes whenever a complete synchronization is achieved, i.e., $\rho_\gamma^*=\lim_{t\to\infty}\rho_\gamma(t)=0$ for $\gamma > \gamma_c$; whilst it remains finite at any time in the desynchronized state, i.e., for $\gamma < \gamma_c$.

The order parameter $\rho_\gamma(t)$ allows us to define the critical exponents θ, β and z which characterize the transition; θ is the exponent that rules the temporal scaling of the order parameter at the critical point $\gamma=\gamma_c$, namely,

$$\rho_{\gamma_c}(t) \sim t^{-\theta}. \tag{8}$$

For $\gamma < \gamma_c$, $\rho_\gamma^* \neq 0$ and one has

TABLE I. Critical exponents for nearest-neighbor coupled tent and Bernoulli maps as well as for the corresponding stochastic models. Also, the best estimations of the critical indices for DP and MN universality classes are reported.

	θ	β	z
Bernoulli	0.159(1)	0.27(1)	1.58(4)
RM ($\Delta=0$)	0.1595(4)	0.276(2)	1.58(2)
DP[a]	0.159464(6)	0.276486(6)	1.580745(6)
Tent	1.275(15)	1.70(8)	1.5(1)
RM ($\Delta=0.2$)	1.13(3)	1.67(3)	1.53(6)
MN[b]	1.10(5)	1.70(5)	1.53(7)
MN[c]	1.184(10)	1.776(15)	⋯

[a]Reference 43.
[b]Reference 49.
[c]Reference 50.

$$\rho_\gamma^* \sim (\gamma_c - \gamma)^\beta, \tag{9}$$

which defines the critical exponent β. Finally, the dynamical exponent z can be defined in terms of the finite-size scaling relation, valid at the critical point,

$$\rho_{\gamma_c}(t) \sim L^{-\theta z} f(t/L^z). \tag{10}$$

These three indices are sufficient to fully characterize the transition, since from their knowledge all the other critical exponents can be derived. In particular, the exponent $\nu_\perp$ (resp. $\nu_\parallel$) ruling the divergence of spatial (resp. temporal) correlation length at the critical point is given by

$$\nu_\perp = \frac{\beta}{\theta z} \quad \left(\text{resp. } \nu_\parallel = \frac{\beta}{\theta}\right). \tag{11}$$

A detailed description of the numerical estimation of θ, β, and z is reported in the following sections.

IV. SHORT-RANGE INTERACTIONS

Let us now consider the synchronization of two replicas of diffusively coupled map lattices. We start with the case of coupled tent maps where the linear analysis is sufficient to identify the critical point and we can thus limit to study the behavior of the difference field $w_i(t)$ in the tangent space. In particular, the norm of this field grows at a rate given by the transverse Lyapunov exponent[3]

$$\lambda_\perp = \lim_{t\to\infty} \|w_i(t)\| = \ln(1-2\gamma) + \Lambda, \tag{12}$$

where Λ is the maximal Lyapunov exponent of a single CML. The synchronization transition occurs at the point where $\lambda_\perp$ vanishes, locating the critical coupling to

$$\gamma_c = \tfrac{1}{2}(1 - e^{-\Lambda}). \tag{13}$$

For this model, it has been suggested that $\gamma_c = 0.176\,15(5)$,[3] by extrapolating from finite size measurements the asymptotic value for Λ. We have estimated the synchronization value from the scaling of the density $\rho_\gamma(t)$ for chains of length $L=2^{25}$ finding $\gamma_c=0.176\,16(2)$, in agreement with the previous estimation. The corresponding critical exponents are reported in Table I, we observe that these values are in reasonable agreement with the one reported in

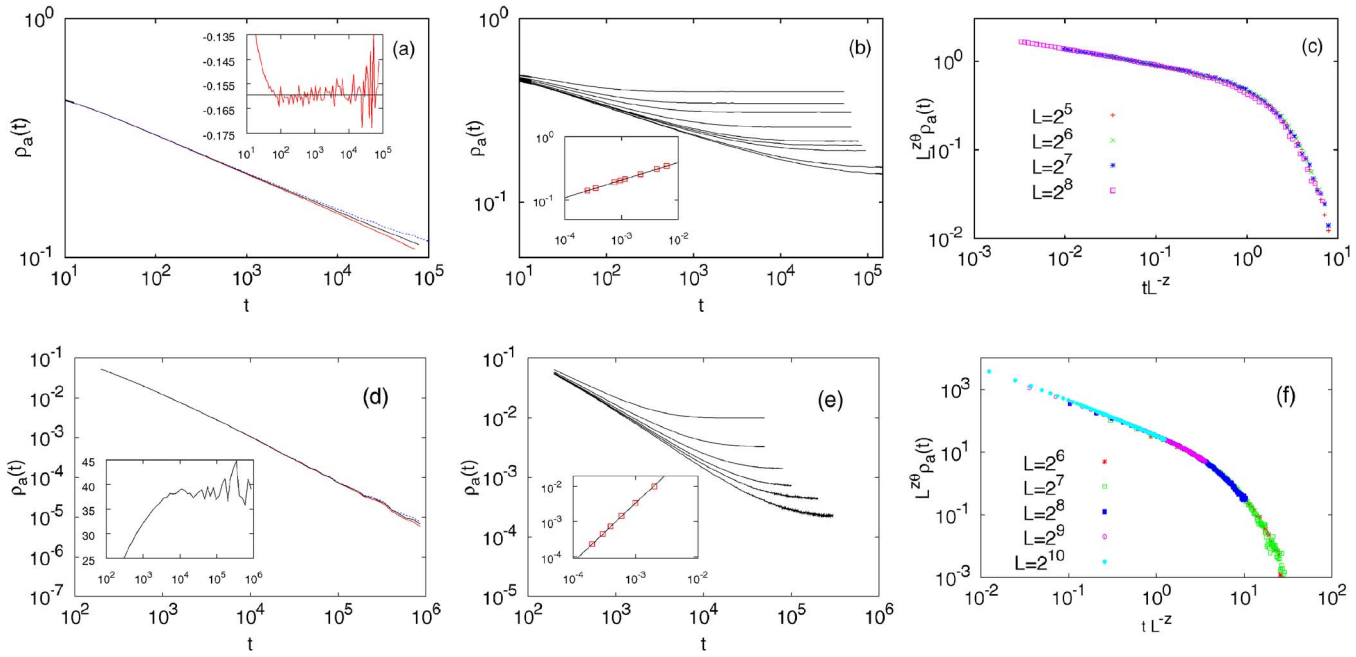

FIG. 2. (Color online) (Top) Scaling relationships for the critical exponents for the random multiplier (RM) models (4) and (5) with NN coupling for $\Delta=0$: (a) $\rho_a(t)$ vs t is displayed for $a=0.606\,20$, $0.606\,15$, $0.606\,10$ with $L=2^{19}$ maps and averaging over 5×10^2 different realizations. The inset shows the logarithmic derivative $d\ln[\rho_a(t)]/d\ln(t)$; (b) various curves $\rho_a(t)$ vs t are reported for $a<a_c$ revealing the saturation to ρ_a^*. In the inset ρ_a^* vs $(a-a_c)$ is reported together with the best fit giving the β estimation. Here, $L=2^{19}$ maps and the average is over 500 realizations; (c) data collapse based on Eq. (10), averaging over 10^3-10^4 initial conditions. (Bottom) Same as the top for the random multiplier model with $\Delta=0.2$: (d) Analogous to (a) for $a=0.566\,938$, $0.566\,942$, $0.566\,945$ with $L=5\times10^5$ and averaging over $1-2\times10^2$ realizations. Here in the inset we report $\rho_{ac}(t)t^\theta$ vs t; (e) same as (b) with $L=5\times10^5$ and averaging over $2^2-1.2\times10^3$ initial conditions; (f) analogous to (c), averaging over 10^5 initial conditions. The values of the estimated critical exponents are reported in Table I.

the literature for the MN universality class,[5,49] apart for θ, which is larger than the corresponding MN value. This difference is probably due to the presence of correlations in the dynamical evolution of these maps, that limits the time range over which a critical scaling of the density $\rho_\gamma(t)$ can be found. In particular, in our analysis as well as in Ref. 3, the time interval where it is possible to observe a clear power-law scaling is limited to $[10^2:4.5\times10^4]$, since at longer times the density (above and below γ_c) always saturates to a (small) constant value. As we show in the following, much more accurate estimations can be obtained by replacing the tent map with its stochastic version, thus reinforcing the hypothesis that scaling laws are hindered by long-time dynamical correlations.

For coupled Bernoulli maps linear analysis fails in locating the synchronization transition, therefore we are forced to directly investigate the scaling of the density $\rho_\gamma(t)$. In particular, for $L=2^{17}$ we have estimated a critical value $\gamma_c=0.287\,52(1)$, in agreement with Ref. 3 (see Table I for the values of the critical exponents). In this case finite size effects and time correlations are less relevant, since good scaling can be already observed in the time interval $[10^2:10^5]$ for much shorter chains.

Let us now turn our attention to the Random Multiplier model (4) and (5), which reproduces the Bernoulli map behavior for $\Delta=0$ and that of a generic continuous map for $\Delta=0.2$.[16,17]

For the stochastic model with $\Delta=0$ the scaling laws are reported in Figs. 2(a)–2(c). In this case the critical point is at $a_c=0.606\,15(5)$ and the measured indices are in perfect agreement with the best estimates of DP's exponents. θ and β coincide with the DP values up to the fourth and third digit, respectively. The evaluation of z is less accurate, since it relies on a data collapse of finite size estimates (10).

In the case $\Delta=0.2$, by considering the scaling in time of the density Eq. (8) for $L=5\times10^5$ maps over a time span $t\in[10^3:10^6]$, we have found that the critical point is located at $a_c=0.566\,942(4)$. In particular, θ has been estimated by a best fit to a power-law over more than two decades [Fig. 2(d)]. The quality of the estimation of the other two exponents can be appreciated from Figs. 2(e) and 2(f). The values of the critical indices are in fairly good agreement with those reported in Ref. 49, obtained by considering a time and space discretized version of the corresponding Langevin equation, i.e., Eq. (6) with $g(n)\propto\sqrt{n}$. It should be remarked that the exponents recently reported in Ref. 50, for a suitable lattice model reproducing the Kardar–Parisi–Zhang-type interface growth, are slightly larger than ours, while the θ value (namely, $\theta=7/6=1.166\bar{6}$) conjectured by Droz and Lipowski[20] is, within the error bars, consistent with our estimation.

V. LONG-RANGE INTERACTIONS

In the presence of long-range interactions, accurate numerical analysis of the synchronization transition requires huge time costs. This can be appreciated by noticing that at each time step $\mathcal{O}(L^2)$ operations are involved [see the cou-

TABLE II. Summary of the results for the critical exponents (also shown in Fig. 3) corresponding to coupled Bernoulli maps and to chains of random multiplier (RM) models (with $\Delta=0$) at various values of σ. HH denotes the results taken from Ref. 40 which are also reported for comparison.

σ	HH			B $q=2$			B $q=4$			B $q=8$			RM $q=4$		
	θ	β	z	θ	β	z	θ	β	z	θ	β	z	θ	β	z
0.2	0.99(4)	0.99(4)	0.21(2)		⋯			⋯			⋯			⋯	
0.5	0.94(4)	0.95(6)	0.54(2)		⋯			⋯		0.97(4)	1.02(5)	0.50(5)	0.92(3)	⋯	⋯
0.6	0.86(4)	0.88(5)	0.58(2)		⋯			⋯			⋯			⋯	
0.8	0.67(3)	0.76(4)	0.71(2)		⋯		0.73(2)	0.91(5)	⋯	0.68(5)	0.80(5)	0.67(5)	0.66(2)	0.76(1)	⋯
1.0	0.52(3)	0.65(3)	0.82(2)		⋯			⋯			⋯		0.52(1)	0.65(1)	0.75(5)
1.1	⋯	⋯	⋯		⋯		0.48(2)	0.64(5)	⋯		⋯			⋯	
1.2	0.40(3)	0.56(3)	0.96(3)	0.50(1)	0.67(5)	0.83(4)	0.40(5)	0.57(4)	0.92(5)		⋯			⋯	
1.4	0.33(3)	0.49(3)	1.09(3)	0.35(1)	0.52(5)	0.96(4)	0.33(5)	0.49(5)	1.05(5)		⋯		0.33(1)	0.48(2)	1.06(4)
1.6	0.27(3)	0.43(3)	1.21(3)	0.30(1)	0.49(5)	1.14(4)		⋯			⋯		0.27(1)	0.41(1)	1.20(4)
1.8	0.24(4)	0.39(3)	1.32(3)		⋯			⋯			⋯			⋯	
2.0	0.21(4)	0.34(3)	1.43(3)	0.19(2)	0.35(5)	1.40(3)	0.20(2)	0.35(3)	1.45(5)		⋯		0.20(1)	0.33(1)	1.42(2)
2.2	0.19(4)	0.32(3)	1.49(4)		⋯			⋯			⋯			⋯	
2.4	0.17(4)	0.30(3)	1.53(5)		⋯			⋯			⋯			⋯	
3.0	⋯	⋯	⋯	0.16(1)	0.29(5)	1.58(4)		⋯			⋯			⋯	
5.0	0.159538	0.276	1.58		⋯			⋯			⋯			⋯	

pling definition in Eq. (3)]. Simulation times become prohibitive as the range of the interaction increases (i.e., the exponent σ decreases), because finite size effects become more relevant and larger sizes are needed. It is therefore fundamental to reduce the CPU cost for each time step. As in Refs. 24 and 36, to achieve such aim we consider the following coupling scheme Eq. (3):

$$\tilde{z}_i = (1-\epsilon)z_i + \frac{\epsilon}{\eta(\sigma)}\left\{(z_{i-1}+z_{i+1}) + \sum_{m=1}^{M}\frac{z_{i-j_m(q)}+z_{i+j_m(q)}}{[j_m(q)]^{\sigma}}\right\}, \tag{14}$$

where $j_m(q)=q^m-1$ and $M=\log_q(L/2)$;[51] the model with full coupling Eq. (3) is recovered for $j_m(q)=m$, $M=L-1$ and by substituting $\sigma\to 1+\sigma$ (see below for more details). Clearly, the new choice is very convenient because each updating step only requires $\mathcal{O}(L\log_q L)$ operations instead of $\mathcal{O}(L^2)$ needed for the fully coupled case. The parameter q is typically chosen as $q=2,4$ and 8, while the normalization factor is given by $\eta(\sigma)=2\{1+\Sigma_{m=1,M}[j_m(q)]^{-\sigma}\}^{-1}$.

The critical properties of the reduced model $[j_m(q)=q^m-1]$ with exponent σ map into those of the fully coupled one $(j_m=m)$ with exponent $\sigma_{fc}=\sigma+1$. This can be easily understood by noticing that the two versions of the model should display the same critical behavior once the spatial interactions scale analogously. For the modified model the coupling weight over the interval $[j_m(q):j_{m+1}(q)]$, containing a single coupled site, is simply given by

$$\frac{1}{j_{m+1}(q)^{\sigma}} \sim \frac{1}{q^{(m+1)\sigma}},$$

while over the same interval the weight for the fully coupled model can be estimated by evaluating the sum

$$\sum_{k=j_m(q)+1}^{j_{m+1}(q)}\frac{1}{k^{\sigma_{fc}}} \sim \frac{1}{q^{(m+1)(\sigma_{fc}-1)}}.$$

By comparing the two expressions it is thus clear that the two weights scale in the same manner when $\sigma_{fc}=\sigma+1$, as we have also numerically verified in Ref. 24. Apart for this shift of the σ value, the fully coupled and reduced model are completely equivalent, as far as their critical properties are concerned, and using the latter is simply a way to reach larger sizes.

Before discussing the numerical results we observe that the coupling scheme (14) can be easily implemented both for coupled maps as well as for the stochastic model.

A. Discontinuous maps and ADP universality class

Synchronization transition of long-ranged coupled systems with discontinuous maps has been previously studied in Ref. 21, as far as the self-synchronization of a single chain is concerned, and in Ref. 24, where the synchronization of two (transversely coupled) replicas is discussed. Here we summarize the results obtained in Ref. 24 for Bernoulli maps coupled with reduced coupling scheme[52] and extend the analysis to the random multiplier model with $\Delta=0$ in the same coupling conditions.

In order to observe clean scaling laws, we have employed the reduced scheme with increasingly larger q values for smaller σ. This amounts to chain lengths varying from $L=2^{16}$ for $\sigma=5.0$ up to $L=2^{22}$ for $\sigma=0.5$. Analogous to the NN case, due to the failure of linear analysis, the critical point γ_c has been located by considering the scaling relation (8), in particular from the critical power-law decay the exponent θ can be estimated. The critical index β can be derived by considering the asymptotic values ρ_{γ}^{*} below the transition $(\gamma<\gamma_c)$ as in Eq. (9), finally z is estimated by data collapse

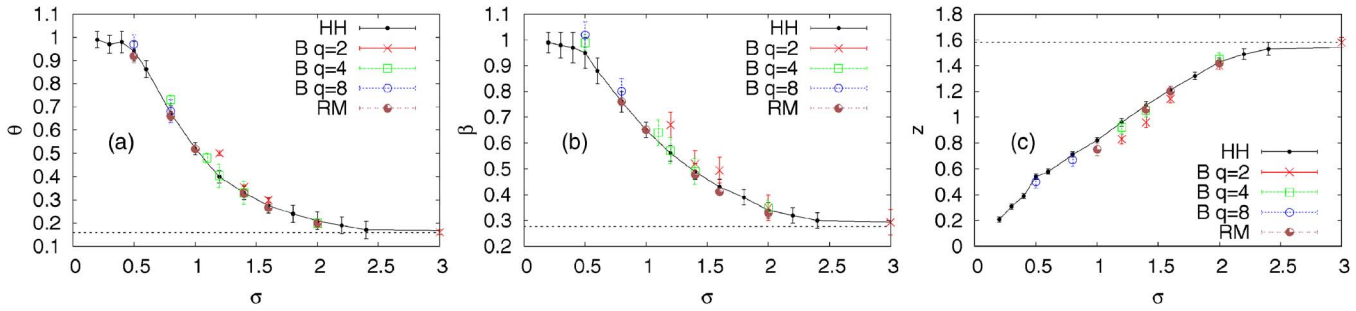

FIG. 3. (Color online) Critical exponents (a) θ, (b) β, and (c) z for coupled Bernoulli maps and random multiplier (RM) models (for $\Delta=0$) as a function of the long-range power exponent σ compared with those obtained in Ref. 40 for a stochastic lattice model. Symbols are explained in the legend. The dotted horizontal line represents the best estimate of the critical exponents for usual DP, i.e., for nearest-neighbor spreading.

based on the finite-size relation (10) at $\gamma=\gamma_c$. As shown in Ref. 24, the quality of the scaling behavior is very good.

Table II and Fig. 3 summarize our findings and present the new critical exponents estimated for the random multiplier model (4) and (5), where we have employed the coupling scheme Eq. (14) with $q=4$ and $M=7$ (for $\sigma=1.4$ and 1.6) and $M=9$ (for $\sigma=1.0$). As one can appreciate from Table II the estimated errors are smaller for the stochastic model than for the Bernoulli map. In Table II we also report the critical indices found by Hinrichsen and Howard[40] for the anomalous DP universality classes which, as one can see, are approached by those obtained with the Bernoulli map at increasing q, i.e., for chains with larger sizes. This tendency suggests that the observed discrepancies are mainly due to finite size effects, which however seem to be less severe for the stochastic model. Indeed by considering the random multiplier model with chain sizes $L\sim 3\times 10^4-5\times 10^5$ we found that the exponents coincide, within the error bars, with those reported in Ref. 40.

According to the analysis reported in Refs. 39 and 40, the upper critical dimension d_c is 2σ and therefore the mean-field regime in the one-dimensional chain should establish below $\sigma_m\equiv 0.5$. The corresponding critical exponents are $\theta_{MF}=\beta_{MF}=1$ and $z_{MF}=\sigma$ (in accordance the temporal and spatial correlation length exponents are given by $\nu_{\|MF}=1$ and $\nu_{\perp MF}=1/\sigma$). Therefore, the long-range nature of the interactions is reflected in the mean-field regime only by the scaling of the spatial correlations, since for short-range interactions the exponents coincide apart $z_{MF}=2$ (and, correspondingly, $\nu_{\perp MF}=1/2$). Our data reported at $\sigma=0.5$ for the Bernoulli maps confirm the mean-field expectations, but due to computational limitations we could not explore smaller σ values.

For ADP, it has also been shown[39,40] that the following hyperscaling relation holds:

$$\delta=1-\sigma+(1-2\theta)z\equiv 0; \tag{15}$$

in the σ-range $[\sigma_m:\sigma_c]$. The σ_c value at which the behavior of the system should cross over to usual DP can be directly estimated by inserting the estimated values of the DP exponents in Eq. (15). Quite astonishingly the crossover takes place at $\sigma_c\equiv 2.0677(2)>2$, as suggested also by field theoretic arguments.[39,40] As shown in Table III the relation (15) is fulfilled within the error bars for the Bernoulli coupled maps as well as for its stochastic version. Notice that, δ departs from zero only at $\sigma=3.0>\sigma_c$, where usual DP scalings are expected. Finally, in the Appendix we show that, after a suitable spatio-temporal coarse-graining, the stochastic model can be effectively described by a Langevin equation of the form Eq. (7) corresponding to the field theoretic description associated with ADP. These results further reinforce the parallel between ST induced by nonlinear effects, in the presence of power-law interactions, and ADP.

B. Continuous maps

Let us finally consider two coupled replicas with local dynamics given by the tent map. In this case the critical point can be estimated by the vanishing of the transverse Lyapunov exponent accordingly to the expression (13). Furthermore, we have independently evaluated γ_c by examining the critical behavior of the density $\rho_\gamma(t)$. Usually the Lyapunov approach was able to locate γ_c within a precision of $1-2\times 10^{-4}$ or even better.

In the present case, to simplify the analysis we keep the parameter $q=4$ and we analyze system sizes ranging from $L=2^{19}$ to $L=2^{23}$. The results for the exponents θ and β are shown in Fig. 4 while z in Fig. 5, we observe that these critical indices for $\sigma\geq 3$ tend to the results reported for the MN universality class (see Table I). For smaller σ values θ and β (resp. z) increase (resp. decreases) and appear to saturate (resp. to vanish) for $\sigma\leq 1$. While the numerical values are completely different from the ADP ones, the general trends are analogous to those observed for coupled Bernoulli maps. This suggests that in the present situation the mean-field value for the indices are $\theta_{MF}\sim 2.2(1)$, $\beta_{MF}\sim 2.6(1)$ and by assuming a linear dependence among z and the power-law exponent one finds that $z_{MF}\sim 0.65(5)\times(\sigma-\sigma_0)$, with $\sigma_0\sim 0.40(5)$. At variance with the mean-field behavior of the ADP case, θ_{MF} and β_{MF} do not coincide, thus suggesting that

TABLE III. Scaling relation (15) for various values of σ, for each measurement the corresponding basis q is reported. For the random multiplier model with $q=4$ we obtained: For $\sigma=1.0$ $\delta=-0.03(2)$, for $\sigma=1.4$ $\delta=-0.04(4)$ and for $\sigma=1.6$ $\delta=-0.05(4)$. The measured δ are compatible with zero in the range $[0.5:2.0677]$. See text for details.

$\sigma[q]$	3.0 [2]	2.0 [4]	1.4 [4]	1.2 [4]	0.8 [8]	0.5 [8]
δ	0.93(6)	−0.13(9)	−0.04(12)	−0.03(10)	−0.04(9)	0.03(9)

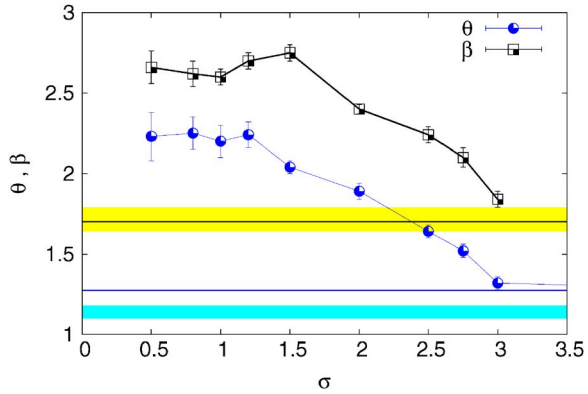

FIG. 4. (Color online) θ and β as a function of σ for the tent map with power-law coupling. The shaded upper (resp. lower) region corresponds to the best estimate of θ (resp. β) reported in the literature (Refs. 5, 20, and 50) for the MN class in the case of short-range interactions. The thick upper (resp. lower) horizontal lines to the corresponding estimates for coupled tent maps with NN coupling reported in Table I. The employed system sizes vary between $L=2^{19}$ and $L=2^{21}$ with $q=4$ for the long-range models. For systems with NN interactions we used sizes $L=2^{25}$ for the θ-estimation and $L=2^{18}$ for β.

$\nu_{\|MF} \sim 1.18(10)$ and z seems to vanish already for $\sigma \sim 0.40(5)$. Finally, from the numerical estimates of z we can conjecture that $\nu_{\perp MF} \sim 1.8(5)/(\sigma-\sigma_0)$. Apart from the poor quality of the estimates, it is important to stress that, analogous to ADP, the presence of long-range interactions reflects mainly in the scaling of the spatial correlations. The mean-field limit for systems with multiplicative noise has been examined recently only for short-range couplings.[54,55] The authors of the papers agree on the values of the correlation exponents $\nu_{\|MF}=1$ and $\nu_{\perp MF}=1/2$, which implies $z_{MF}=2$ and $\theta_{MF}=\beta_{MF}$. However, the value of θ_{MF} seems to depend on the approximation employed to derive the mean-field. In particular, in Refs. 54 and 56 a value $\theta_{MF}=5/3$ is reported, while in Refs. 5 and 55 is predicted that θ_{MF} is a nonuniversal scaling exponent dependent on noise amplitude, diffusion coefficient, and nonlinear term. Therefore the mean-field analysis is still unclear for the multiplicative noise case with usual diffusion (as discussed also in Ref. 55) moreover a study for the fractional diffusion case is still to be addressed.

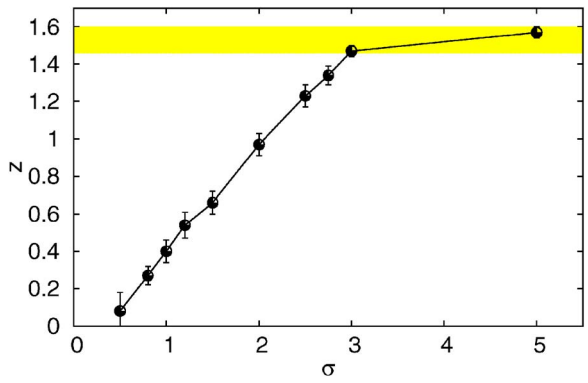

FIG. 5. (Color online) z vs σ for the tent map with power-law coupling. The shaded region corresponds the best estimate of z reported in the literature (Ref. 5) for the MN class in the case of short-range interactions. For the finite-size scaling chains of length $L=2^4-2^{15}$ have been employed.

The analysis of the corresponding stochastic model, i.e., the random multiplier model with $\Delta=0.2$ with power-law coupling, reveal enormous fluctuations in the asymptotic behavior of the density induced by abrupt synchronizations of the whole chain. Thus making impossible any estimation of critical scaling laws, even by employing quite long chains (namely, $L=2^{23}$). Our analysis cannot rule out the possibility that for this stochastic model the transitions became discontinuous. Similar to what done in Ref. 53, a detailed analysis of the scaling of the synchronized clusters with the system size should be performed to address this point, but this goes beyond our scopes. Moreover, it is quite astonishing that the analysis of the deterministic case was somehow clearer. We can conjecture that the correlations induced by the deterministic evolution of coupled tent maps prevent the abrupt synchronization of large islands within the chain. However, this is just a working hypothesis to be investigated in the future.

VI. CONCLUSIONS

The critical properties of the synchronization transitions among replicas of chaotic and stochastic spatially extended systems have been numerically estimated both for diffusively coupled and for power-law interacting systems. In particular, we focus on the differences between transitions dominated by linear and nonlinear mechanisms.

For nearest-neighbor coupling, our analysis confirms previous findings indicating that the transitions are always continuous, while two distinct universality classes characterize the transition depending on the nature of the local dynamics. For continuous (resp. discontinuous) local maps the critical properties correspond to those of multiplicative noise (resp. directed percolation) nonequilibrium phase transitions.

The introduction of a power-law coupling modifies the critical properties of the STs, in particular for (quasi-) discontinuous maps all the studied transitions can be gathered in a unique family of universality classes termed anomalous directed percolation. The analysis of the stochastic models reinforce the analogy between epidemic spreading mediated by unrestricted Lévy flights and the examined STs for a twofold reason: On one side the numerically evaluated indices are almost identical to the ones found in Ref. 40 for a lattice model reproducing anomalous DP, on the other hand an effective Langevin equation has been derived coinciding with that proposed for ADP. It is worth stressing that it is highly nontrivial that the deterministic systems here investigated exhibit scaling properties in quantitative agreement with those found for stochastic models, like the lattice model studied in Ref. 40 and the random multiplier model. Moreover, the accuracy achieved in the investigation of the STs for the stochastic model suggests that these models can represent a valid alternative to the use of lattice dynamics for the investigations of nonequilibrium phase transitions.

The study of smooth continuous maps has revealed a behavior of the critical exponents similar to the one observed for ADP, namely, the indices vary with continuity with the power exponent σ, albeit their values are different from those found for ADP. Moreover, the estimated exponents do not correspond to any known universality class and this represents a challenge for future theoretical investigations. In

particular, the natural candidate to explore is the field equation (7) with noise amplitude $g(n) \propto n$ in order to understand if an anomalous multiplicative noise class could be defined.

ACKNOWLEDGMENTS

We thank F. Ginelli for continuous and fruitful exchanges and M. Muñoz for useful discussions. C.J.T. acknowledges financial support by SBF (Switzerland) through research project C05.0148 (Physics of Risk).

APPENDIX: FIELD DESCRIPTION FOR THE RANDOM MULTIPLIER MODEL

The aim of this appendix is to provide a self-contained heuristic derivation of the field equation associated with the ST for spatially extended systems with power-law decaying interactions, where the transition is controlled by finite amplitude effects. In particular, we focus on the random multiplier model (4) for $\Delta=0$, which closely reproduces the ST for discontinuous (or quasi-discontinuous) coupled maps. In our derivation we follow Ref. 17 where, by introducing a suitable spatio-temporal coarse-graining, it has been shown that the nearest-neighbor version of the model can be "effectively" described by the Reggeon field theory associated with ordinary DP. In the following, we show that the power law coupled version of the model can be reduced to Eq. (6), which was proposed in Ref. 40 to describe ADP in an epidemic spreading processes mediated by Lévy flights.

For the fully coupled case, the model (4) can be rewritten as follows:

$$v_i(t) = (1 + \nabla_\epsilon^2 + \nabla_\epsilon^\sigma) w_i(t), \tag{A1}$$

where v_i plays the role of $\tilde{w}_i$ and ∇_ϵ^2 is the discretized Laplacian operator,

$$\nabla_\varepsilon^2 w_i(t) = \frac{\varepsilon}{2} w_{i+1}(t) + \frac{\varepsilon}{2} w_{i-1}(t) - \varepsilon w_i(t), \tag{A2}$$

while ∇_ϵ^σ represents a discretized fractional derivative, which corresponds to the most relevant term in the small momentum expansion of the following discretized convolution sum:

$$\nabla_\epsilon^\sigma w_i(t) \sim \frac{\epsilon}{\eta'(\sigma)} \sum_{m=2}^{M} \frac{w_{i-m} + w_{i+m}}{m^{\sigma+1}}. \tag{A3}$$

Notice that the sum already contains a short distance cutoff that should be anyway considered to have a meaningful definition of fractional derivatives.[39,40] The stochastic variable $w_i(t) \in [0:1]$ evolves according to Eq. (4), and the positive parameter ϵ represents the amplitude of the spatial coupling. The constant $\eta'(\sigma)=2\Sigma_{m=2}^{M}(m)^{-\sigma-1}$ is a normalization factor. Periodic boundary conditions are imposed.

Let us formally rewrite Eq. (4) as

$$w_i(t+1) = 2a v_i(t) - a^2 v_i^2(t) + g(v)\xi_i'(t), \tag{A4}$$

where the term ξ_i' represents a zero-average δ-correlated noise term with unitary variance. In order to recognize that the above expression recovers the original model it is enough to notice that

$$\xi_i'(t) = \frac{1}{g(v)}[\xi_v(i,t) - \langle \xi_v(i,t) \rangle], \tag{A5}$$

ξ_v being the dicotomic noise term

$$\xi_v(i,t) = \begin{cases} 1, & \text{w.p. } p = a v_i(t) \\ a v_i(t), & \text{w.p. } 1-p, \end{cases} \tag{A6}$$

whose average $\langle \xi_v \rangle$ and variance $g^2(v)$ have the following expressions: $\langle \xi_v \rangle = (2a-1)v - a^2 v^2$ and $g^2(v) = av - 3a^2v^2 + 3a^3v^3 - a^4v^4$ (for details, see Ref. 17).

We can now introduce a coarse-grained variable $n(x,t) = \bar{w}_i(t)$ (where the bar denotes an average over a suitable space-time cell), in terms of which Eq. (A1) can be written as

$$\bar{v}_i(t) = n(x,t) + \frac{\epsilon}{2}\nabla^2 n(x,t) + \frac{c(\epsilon)}{2}\nabla^\sigma n(x,t),$$

where the constant $c(\varepsilon)$ takes into account the presence of the cutoff and various normalization factors. The coarse-grained evolution equation is then derived from Eq. (A4) and reads

$$\begin{aligned} \partial_t n(x,t) = {} & (2a-1)n(x,t) + a\varepsilon\nabla^2 n(x,t) + ac(\varepsilon)\nabla^\sigma n(x,t) \\ & - a^2 n^2(x,t) - \frac{a^2}{4}[\varepsilon\nabla^2 n(x,t) + c(\varepsilon)\nabla^\sigma n(x,t)]^2 \\ & - a^2 n(x,t)[\varepsilon\nabla^2 n(x,t) + c(\varepsilon)\nabla^\sigma n(x,t)] \\ & + g\left[n(x,t) + \frac{\epsilon}{2}\nabla^2 n(x,t) + \frac{c(\epsilon)}{2}\nabla^\sigma n(x,t) \right]\rho(x,t), \end{aligned} \tag{A7}$$

where the coarse-grained noise term $\rho(x,t)$ is Gaussian and space-time δ correlated. In proximity of the transition the terms of order $(\nabla^2 n)^2$, $(\nabla^\sigma n)^2$, $n\nabla^2 n$, and $n\nabla^\sigma n$ can be shown to be irrelevant, and also the terms $\sqrt{\nabla^2 n}$ and $\sqrt{\nabla^\sigma n}$ entering in the noise amplitude $g(\ldots)$.

By discarding the irrelevant terms one obtains

$$\begin{aligned} \partial_t n = {} & [(2a-1) + a\varepsilon\nabla^2 + ac(\varepsilon)\nabla^\sigma] n(x,t) - a^2 n^2(x,t) \\ & + \sqrt{an}\rho(x,t) \end{aligned} \tag{A8}$$

that is essentially the same Langevin equation proposed to describe anomalous DP in Refs. 39 and 40.

[1] A. S. Pikovsky, M. Rosenblum, and J. Kurths, *Synchronization. A Universal Concept in Nonlinear Sciences* (Cambridge University Press, Cambridge, 2001).

[2] L. Baroni, R. Livi, and A. Torcini, in *Dynamical Systems: From Crystal to Chaos*, edited by J. M. Gambaudo, P. Hubert, P. Tisseur and S. Vaienti (World Scientific, Singapore, 2000), p. 23; L. Baroni, R. Livi, and A. Torcini, Phys. Rev. E **63**, 036226 (2001).

[3] V. Ahlers and A. S. Pikovsky, Phys. Rev. Lett. **88**, 254101 (2002).

[4] H. Hinrichsen, Adv. Phys. **49**, 815 (2000).

[5] M. A. Muñoz, in *Advances in Condensed Matter and Statistical Mechanics*, edited by E. Korutcheva and R. Cuerno (Nova, New York, 2004).

[6] H. Fujisaka, Prog. Theor. Phys. **70**, 1264 (1983); H. Fujisaka and T. Yamada, *ibid.* **69**, 32 (1983).

[7] L. M. Pecora and T. L. Carroll, Phys. Rev. Lett. **64**, 821 (1990); Phys. Rev. A **44**, 2374 (1991).

[8] G. D. Van Wiggeren and R. Roy, Science **279**, 1198 (1998); A. Argyris, D. Syvridis, L. Larger, V. Annovazzi-Lodi, P. Colet, I. Fischer, J. García-Ojalvo, C. R. Mirasso, L. Pesquera, and K. A. Shore, Nature (London) **438**, 343 (2005).

[9]D. J. DeShazer, R. Breban, E. Ott, and R. Roy, Phys. Rev. Lett. **87**, 044101 (2001).
[10]W. Wang, I. Z. Kiss, and J. L. Hudson, Chaos **10**, 248 (2000).
[11]E. Mosekilde, Y. Maistrenko, and D. Postnov, *Chaotic Synchronization: Applications to Living Systems* (World Scientific, Singapore, 2002).
[12]V. Makarenko and R. Llinás, Proc. Natl. Acad. Sci. U.S.A. **95**, 15747 (1998).
[13]M. C. Cross and P. H. Hohenberg, Rev. Mod. Phys. **65**, 851 (1993).
[14]F. Bagnoli, L. Baroni, and P. Palmerini, Phys. Rev. E **59**, 409 (1999).
[15]F. Bagnoli and F. Cecconi, Phys. Lett. A **260**, 9 (2001).
[16]F. Ginelli, R. Livi, and A. Politi, J. Phys. A **35**, 499 (2002).
[17]F. Ginelli, R. Livi, A. Politi, and A. Torcini, Phys. Rev. E **67**, 046217 (2003).
[18]M. A. Muñoz and R. Pastor-Satorras, Phys. Rev. Lett. **90**, 204101 (2003).
[19]F. Ginelli, V. Ahlers, R. Livi, D. Mukamel, A. S. Pikovsky, A. Politi, and A. Torcini, Phys. Rev. E **68**, 065102(R) (2003).
[20]M. Droz and A. Lipowski, Phys. Rev. E **67**, 056204 (2003); **68**, 056119 (2003).
[21]M. Cencini and A. Torcini, Physica D **208**, 191 (2005).
[22]F. Bagnoli and R. Rechtman, Phys. Rev. E **73**, 026202 (2006).
[23]P. M. Gade and C.-K. Hu, Phys. Rev. E **73**, 036212 (2006).
[24]C. J. Tessone, M. Cencini, and A. Torcini, Phys. Rev. Lett. **97**, 224101 (2007).
[25]P. Grassberger, *Directed Percolation: Results and Open Problems*, in "Nonlinearities in Complex Systems," edited by S. Puri and S. Dattagupta (Narosa, New Delhi, 1997).
[26]K. Kaneko, Prog. Theor. Phys. **72**, 980 (1984).
[27]A necessary condition to observe information propagation, even for negative transverse Lyapunov exponent, is that the value of the slope of the considered map should be quite large, but it is not strictly necessary that the map is discontinuous (Refs. 28 and 29). In this sense, the term should be interpreted as quasi-discontinuous.
[28]M. Cencini and A. Torcini, Phys. Rev. E **63**, 056201 (2001).
[29]A. Torcini, P. Grassberger, and A. Politi, J. Phys. A **28**, 4533 (1995).
[30]P. Grassberger, Phys. Rev. E **59**, R2520 (1999).
[31]L. Hufnagel, D. Brockmann, and T. Geisel, Proc. Natl. Acad. Sci. U.S.A. **101**, 15124 (2004); D. Brockmann, L. Hufnagel, and T. Geisel, Nature (London) **439**, 462 (2006).
[32]M. Dharmala, V. K. Jirsa, and M. Ding, Phys. Rev. Lett. **92**, 028101 (2004).
[33]K. Wiesenfeld, P. Colet, and S. H. Strogatz, Phys. Rev. Lett. **76**, 404 (1996).
[34]C. Peskin, *Mathematical Aspects of Heart Physiology* (Courant Institute of Mathematical Sciences, New York University, New York, 1975).
[35]G. Paladin and A. Vulpiani, J. Phys. A **25**, 4911 (1994); A. Torcini and S. Lepri, Phys. Rev. E **55**, R3805 (1997).
[36]A. Torcini, in *Chaos: The Interplay Between Stochastic and Deterministic Behavior*, Lecture Notes in Physics, edited by P. Garbaczewski, M. Wolf, and A. Weron (Springer Verlag, Berlin, 1995), Vol. 457, p. 537.
[37]C. Anteneodo, S. E. de S. Pinto, A. M. Batista, and R. L. Viana, Phys. Rev. E **68**, 045202(R) (2003).
[38]H. Hinrichsen, J. Stat. Mech.: Theory Exp. **2007**, P07066.
[39]H. K. Janssen, K. Oerding, F. van Wijland, and H. J. Hilhorst, Eur. Phys. J. B **7**, 137 (1999).
[40]H. Hinrichsen and M. Howard, Eur. Phys. J. B **7**, 635 (1999).
[41]D. Mollison, J. R. Stat. Soc. Ser. B (Methodol.) **39**, 283 (1977); P. Grassberger, in *Fractals in Physics*, edited by L. Pietronero and E. Tosatti (Elsevier, New York, 1986).
[42]K. Kaneko, Phys. Rev. Lett. **63**, 219 (1989); K. Kaneko, Physica D **41D**, 137 (1990).
[43]I. Jensen, J. Phys. A **32**, 5233 (1999).
[44]P. Rupp, R. Richter, and I. Rehberg, Phys. Rev. E **67**, 036209 (2003).
[45]K. A. Takeuchi, M. Kuroda, H. Chaté, and M. Sano, Phys. Rev. Lett. **99**, 234503 (2007).
[46]A. S. Pikovsky and J. Kurths, Phys. Rev. E **49**, 898 (1994).
[47]M. Kardar, G. Parisi, and Y.-C. Zhang, Phys. Rev. Lett. **56**, 889 (1986).
[48]H. Hinrichsen, R. Livi, D. Mukamel, and A. Politi, Phys. Rev. Lett. **79**, 2710 (1997).
[49]Y. Tu, G. Grinstein, and M. A. Muñoz, Phys. Rev. Lett. **78**, 274 (1997).
[50]T. Kissinger, A. Kotowitz, O. Kurz, F. Ginelli, and H. Hinrichsen, J. Stat. Mech.: Theory Exp. **2005**, P06002.
[51]It should be noticed that, only for $q=2$, the sum in Eq. (14) should be slightly modified in order to avoid an overlap with the diffusive term. In particular, the sum should start with $m=2$ and not $m=1$.
[52]In Ref. 24 and for the results here reported for the Bernoulli map, we used a slightly different modified coupling, namely, $\tilde{z}_i=(1-\epsilon)z_i + \epsilon/\eta(\sigma)\sum_{m=1}^{M} z_{i-j_m(q)}+z_{i+j_m(q)}/[j_m(q)]^{\sigma}$ with $j_m(q)=q^m-1$, which coincides with Eq. (14) only for $q=2$. For $q\neq 2$ the above coupling scheme does not include a diffusive interaction. Several tests, however, have shown that the scaling laws obtained by employing the two coupling schemes are essentially coincident.
[53]F. Ginelli, H. Hinrichsen, R. Livi, D. Mukamel, and A. Politi, Phys. Rev. E **71**, 026121 (2005).
[54]F. Ginelli and H. Hinrichsen, J. Phys. A **37**, 11085 (2004).
[55]M. A. Muñoz, F. Colaiori, and C. Castellano, Phys. Rev. E **72**, 056102 (2005).
[56]Due to a misprint, the wrong value $\theta_{MF}=4/3$ is reported in Ref. 54, F. Ginelli (private communication, 2008).